Available online at www.sciencedirect.com
ScienceDirect
Catalysis Today 124 (2007) 156–162
CATALYSIS TODAY
www.elsevier.com/locate/cattod

Photocatalytic oxidation of methyl parathion over TiO_2 and ZnO suspensions

Eleni Evgenidou [a,*], Ioannis Konstantinou [b], Konstantinos Fytianos [a], Ioannis Poulios [c], Triantafyllos Albanis [d]

[a] *Environmental Pollution Control Laboratory, Chemistry Department, Aristotle University of Thessaloniki, Greece*
[b] *Department of Environmental and Natural Resources Management, University of Ioannina, 30100 Agrinio, Greece*
[c] *Laboratory of Physical Chemistry, Chemistry Department, Aristotle University of Thessaloniki, 54124 Thessaloniki, Greece*
[d] *Department of Chemistry, University of Ioannina, 45110 Ioannina, Greece*

Available online 7 May 2007

Abstract

The photocatalytic degradation of methyl parathion in aqueous solutions, using two different photocatalysts (TiO_2 and ZnO) has been investigated. The degradation of methyl parathion follows first order kinetics according to the Langmuir–Hinshelwood model. Complete degradation is achieved within 45 or 150 min when treated with illuminated TiO_2 or ZnO, respectively. It was observed that the initial rate increases linearly with an increase of the amount of catalyst up to a level where it reaches a plateau corresponding to the optimum of light absorption. The addition of an oxidant ($K_2S_2O_8$) leads to an increase in the rate of photooxidation. Moreover, illuminated TiO_2 suspensions were proved to be more effective in mineralizing the insecticide compared to ZnO suspensions. Measurements of phosphate, sulfate and nitrate ions gave valuable information about how this process is achieved. Addition of the oxidant enhances mineralization for both photocatalytic systems. Up to eight by-products were identified by GC–MS technique during the photocatalytic degradation of the insecticide that proceeds via oxidation, hydroxylation, dealkylation and hydrolysis of the ester group reaction pathways. Finally, the toxicity of the treated solution was reduced only in the presence of TiO_2, while ZnO suspensions appear to increase the toxicity due to photo-dissolution of ZnO releasing zinc in the treated solution.

Keywords: Methyl parathion; Mineralization; Photocatalysis; TiO_2; Toxicity; ZnO

1. Introduction

Advanced oxidation processes (AOPs) have been efficiently applied on the degradation of a variety of organic contaminants [1–6]. These processes include technologies such as O_3, O_3/UV, H_2O_2/UV, Fenton, photo-Fenton, TiO_2/UV, etc. which are characterized by a common factor: the generation of hydroxyl radicals. These radicals show little selectivity of attack and are able to oxidize a variety of organic compounds due to their high oxidative capacity (reduction potential of $OH^\bullet$ $E_o = 2.8$ V) [1]. The versatility of the AOPs is also enhanced by the fact that they can offer different possible ways for $OH^\bullet$ radicals production, thus, allowing a better compliance with the specific treatment requirements.

Heterogeneous photocatalysis is a very promising technique as it has already been applied with success on the degradation of different categories of organic compounds combining the low cost, the mild conditions and the possibility of using sunlight as the source of irradiation [4]. This technique is based on the illumination of semiconductor particles usually suspended in aqueous solutions. The illumination of these particles with light energy greater than the bandgap energy leads to the production of high energy electron–hole pairs (e^-/h^+), which can migrate to the surface of the photocatalyst and can either recombine producing thermal energy or participate in redox reactions with the compounds that are adsorbed on the photocatalyst's surface, thus, leading to complete mineralization of the organic compounds [3].

In this study, the photocatalytic degradation of methyl parathion has been investigated using TiO_2 and ZnO as catalysts. Methyl parathion is a non-systemic insecticide that is being used in many countries worldwide and it is comprised in

* Corresponding author. Tel.: +30 2310997799; fax: +30 2310997873.
E-mail address: evgenidou@gmail.com (E. Evgenidou).

0920-5861/$ – see front matter
doi:10.1016/j.cattod.2007.03.033

the category of organophosphorus pesticides. It is used as a fumigant and acaricide and as a pre-harvest soil and foliage treatment for a wide variety of crops, both outdoors and in greenhouses [7]. It is acutely toxic to mammals, acting by inhibiting the enzyme acetylcholinesterase (AChe) in nerve tissue [8].

The objectives of this study were to evaluate the kinetics of pesticide disappearance, to examine the influence of various parameters such as the mass of catalyst or the addition of an oxidant and finally to evaluate the extend of mineralization along with the identification of reaction intermediates that are produced during treatment. Examination of the changes in toxicity during photocatalysis was also necessary as it can provide an overall evaluation of the efficiency of the process used.

The degradation of parathion using TiO_2 photocatalysis has been previously investigated [9–12]. However, no significant effort has been made in evaluating the photocatalytic efficiency of ZnO on parathion's oxidation and the factors affecting it. Moreover, the examination of four different reacting systems (based on combinations between two photocatalysts and an oxidant) in order to evaluate their ability to mineralize parathion and to detoxify the treated solution is first presented in this study.

2. Materials and methods

Methyl parathion analytical grade (99.9% purity) was purchased from Riedel-de-Haen (Germany). HPLC-grade solvents (acetonitrile and water) were supplied by Merck (Darmstadt, Germany). $K_2S_2O_8$ was purchased from Merck. Titanium dioxide P25 Degussa (anatase/rutile: 65/35, non-porous, mean size 30 nm, surface area 56 $m^2\,g^{-1}$) and ZnO (mean size 110 nm, surface area 9.5 $m^2\,g^{-1}$) were used as received. Stock solutions of methyl parathion (40 mg L^{-1}) were prepared in water, protected from light and stored at 4 °C.

Irradiation experiments were carried out in a 500 mL Pyrex UV reactor equipped with a diving Philips HPK 125 W high-pressure mercury lamp. The lamp was jacked with a water-cooled Pyrex filter restricting the transmission of wavelengths bellow 290 nm. The tap water cooling circuit maintained the temperature at 30–35 °C. Insecticide solution (10 mg L^{-1}, unless otherwise stated) with the appropriate amount of catalyst was magnetically stirred before and during the illumination. The pH was not adjusted. At specific time intervals, samples were withdrawn from the reactor. In order to remove the TiO_2 or ZnO particles, the solution samples were filtered through a 0.45 μm filter.

Pesticide concentrations were determined by a Shimadzu 10AD liquid chromatograph equipped with a variable wavelength UV detector using a 250 mm × 4.6 mm, C18 nucleosil 100-S column. The mobile phase was a mixture of acetonitrile and water (60/40, v/v) with a flow rate of 1 mL min^{-1}. The detection was realized at 270 nm. In order to evaluate the extend of mineralization, total organic carbon (TOC) measurements were carried out by a Shimadzu V-csh TOC analyzer. Sulfate, nitrate and phosphate ions were analyzed spectrophotometrically using cuvette tests supplied by WTW (Germany). Toxicity measurements were carried out using the Microtox test measuring the inhibition of bioluminescence of *Vibrio ficheri* at 5 and 15 min of time exposure. Adjustment of the osmotic pressure of the samples in order to obtain salinity 2% and of the pH to 7 ± 1 was carried out prior to analysis.

For the identification of the reaction intermediates the SPE method was applied to the samples previous to analysis using Envicarb extraction cartridges (non-porous GCB, 40–100 μm particle size, 100 $m^2\,g^{-1}$ surface area; Supelco, Bellefonte, PA, USA). The cartridges were conditioned by elution with 2 mL × 4 mL of dichloromethane–methanol (80: 20, v/v) and next, 2 mL × 6 mL of water, acidified to pH 2. After the passage of water samples, the cartridges were vacuum-dried to remove traces of water. Elution of the analytes was conducted with 2 mL × 4 mL of dichloromethane–methanol (80:20, v/v). The eluate was evaporated to dryness, at room temperature, under a light stream of nitrogen and finally dissolved again, with sonication, in ethyl acetate. The volume of the sample prior to injection was adjusted to 1 mL.

GC–MS analyses were performed on a Shimadzu QP 5000 instrument, equipped with a DB 5-MS column (J & W Scientific) of 30 m length and 0.25 i.d., coated with 5% phenyl 95% methylpolysiloxane. Separation of the by-products was conducted under the following chromatographic conditions: injector temperature 240 °C, oven temperature program 55 °C ramped at 5 °C/min to 200 °C followed by another ramp of 1 °C/min to 210 °C, held for 2 min and finally, to 270 °C at 20 °C/min (held for 3 min). Helium was used as carrier gas at a flow of 1 mL min^{-1}. The temperatures of the ion source and the interface were set at 240 and 290 °C, respectively. The MS operated in electron ionization mode with a potential of 70 eV and the spectra were obtained at a scan range from *m/z* 50–450 (full scan mode). The scan time was 47 min and 1.0 μL injections were made.

3. Results and discussion

3.1. Primary degradation

The photocatalytic degradation of methyl parathion in the presence or in the absence of the photocatalysts (TiO_2 or ZnO) is presented in Fig. 1. Complete degradation of the insecticide is achieved within 45 min in the presence of titanium dioxide while in the presence of the same quantity of ZnO complete degradation of methyl parathion is achieved after 150 min. On the other hand, low degradation (∼18% reduction) of the target compound achieved after 2 h of irradiation indicating that the rapid decomposition which is achieved in the presence of the semiconductors can be clearly ascribed to the catalysts' activity. Moreover, blank experiments with the addition of the semiconductors and the absence of irradiation had a negligible effect on the concentration of methyl parathion indicating a negligible adsorption of the insecticide on the catalysts' surface.

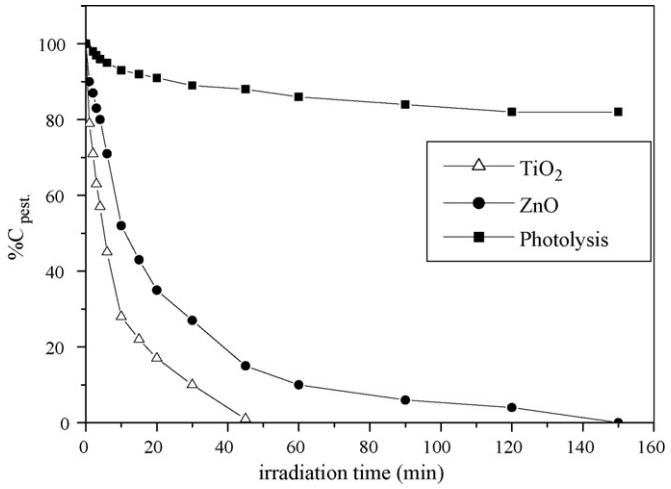

Fig. 1. Photodegradation of methyl parathion in the presence of TiO_2 (100 mg L^{-1}), ZnO (100 mg L^{-1}) or UV light only.

Finally, it is observed that titanium dioxide (TiO_2-P25) is more effective than zinc oxide since more rapid decomposition is achieved, which is in agreement with previous studies [13–15].

3.2. Effect of the concentration of the catalyst

In order to study the effect of the catalyst's concentration on the photodegradation rate of the selected insecticide, experiments were conducted employing different concentrations of TiO_2 and ZnO varying from 10 to 1000 mg L^{-1} (Fig. 2).

Obviously, when low concentrations of the semiconductor are used, increase of the concentration of the catalyst causes increase to the initial reaction rate up to a value where it reaches a plateau. This concentration corresponds to the optimum of light absorption above which light scattering starts to take place [16–19]. Furthermore, at high concentrations of the catalyst agglomeration (particle–particle interactions) can also take place resulting to the loss of surface area available for light absorption [20]. According to Fig. 2, the optimum concentration of titanium dioxide is 200 mg L^{-1} while for zinc oxide is 500 mg L^{-1}. The difference between the two catalysts can be ascribed to the difference of their characteristics like the surface area, the particle size, the electron–hole recombination rate, etc. [20,21]. Consequently, comparison between them was not possible.

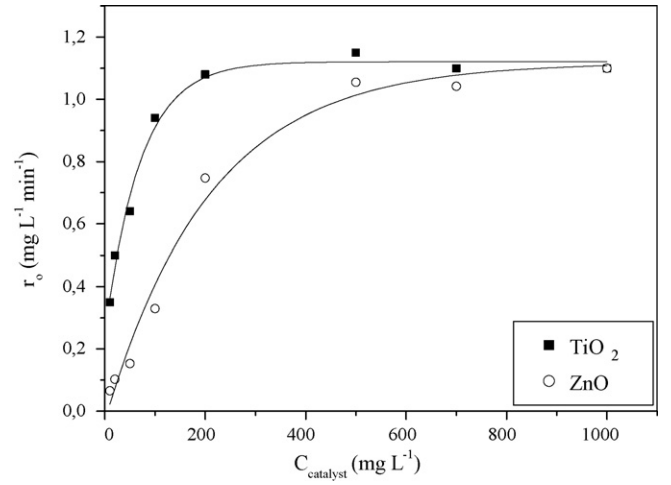

Fig. 2. Dependence of the initial photodegradation rate r_o on the concentration of the catalyst.

3.3. Kinetics

According to many researchers, the influence of the initial concentration of the solute on the photocatalytic degradation rate of the most organic compounds is described by pseudo-first order kinetics which is rationalized in terms of the Langmuir–Hinshelwood model, modified to accommodate reactions occurring at a solid–liquid interface [14,15,22,23]. On the assumption of no competition with reaction by-products, the simplest representation for the rates of disappearance of methyl parathion is given by:

$$r_0 = -\frac{dC}{dt} = \frac{k_r K C_0}{(1 + KC_0)}$$

where r_0 is the initial rate of disappearance (mg L^{-1} min^{-1}) of methyl parathion, C_0 (mg L^{-1}) its initial concentration, K the equilibrium adsorption constant of methyl parathion and k_r reflects the limiting reaction rate at maximum coverage for the experimental conditions. A standard means of using this equation is to demonstrate linearity of data when plotted as the inverse initial rate versus inverse initial concentration:

$$\frac{1}{r_0} = \frac{1}{k_r} + \frac{1}{k_r K}\frac{1}{C_0}$$

Experiments were carried out using various initial concentrations of methyl parathion (5–50 mg L^{-1}) and the r_0 values were independently obtained from the degradation curves, by the linear fit using only the experimental data obtained during the first 10 min of illumination in order to minimize variations as a result of competitive effects of intermediates, pH changes, etc.

As indicated in Fig. 3, the plot of the reciprocal initial rate r_0^{-1} as a function of the reciprocal initial concentration ${C_0}^{-1}$ yields a straight line. The linear transform of this expression yields $k_r = 4.9$ mg L^{-1} min^{-1} (1.9×10^{-5} M min^{-1}) and $K = 0.02$ mg^{-1} L (5.8×10^3 M^{-1}) for the TiO_2 and $k_r = 2.8$ mg L^{-1} min^{-1} (1.1×10^{-5} M min^{-1}) and $K = 0.06$ mg^{-1} L L (1.6×10^4 M^{-1}) for the ZnO.

3.4. Effect of the addition of an oxidant

According to previous studies, the addition of an oxidant to a photocatalytic system enhances the reaction rate. This phenomenon is attributed to the entrapment of the photogenerated electron, thus, preventing the recombination between electrons and holes. The oxidant that is usually tested is hydrogen peroxide and it has been used with success for the

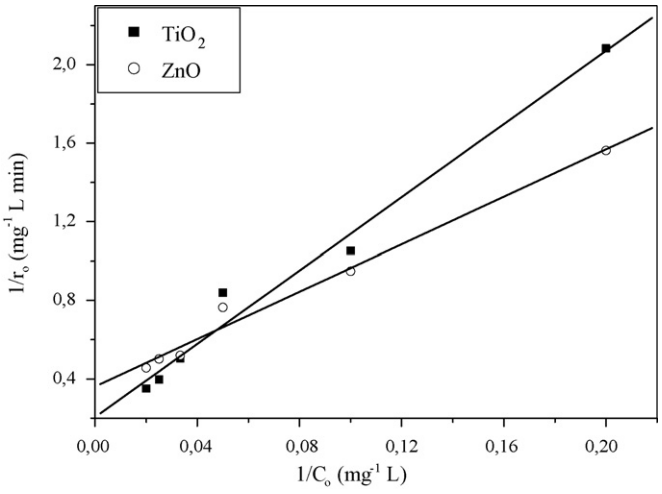

Fig. 3. Linearized reciprocal kinetic plot for the photocatalytic degradation of methyl parathion in the presence of (■) TiO_2 = 100 mg L^{-1} and (○) ZnO = 500 mg L^{-1}.

increase of the photodegradation rate of many organic compounds [23–26].

In this study, the effect of peroxydisulfate is being investigated. This electron scavenger has been tested with success causing an increase to the reaction rate [14,15]. This ability of peroxydisulfate is not only attributed to the promotion of charge separation but also to the production of sulfate radicals which are very strong oxidizing agents according to the following equations [24]:

$$S_2O_8^{2-} + e^- \rightarrow SO_4^{2-} + SO_4^{\bullet -} \quad (1)$$

$$SO_4^{\bullet -} + e^- \rightarrow SO_4^{2-} \quad (2)$$

$$SO_4^{\bullet -} + H_2O \rightarrow SO_4^{2-} + OH^{\bullet} + H^+ \quad (3)$$

$$SO_4^{\bullet -} + RH \rightarrow \cdots \rightarrow SO_4^{2-} + CO_2 \quad (4)$$

The effect of peroxydisulfate on the photocatalytic degradation rate of methyl parathion is presented in Fig. 4.

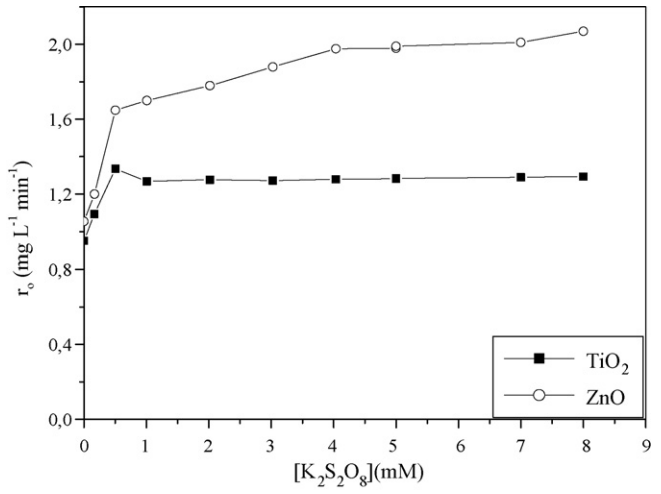

Fig. 4. Effect of the $K_2S_2O_8$ on the photocatalytic degradation rate of methyl parathion in the presence of TiO_2 (100 mg L^{-1}) and ZnO (500 mg L^{-1}).

It is obvious that increase of the oxidant's concentration causes increase to the reaction rate, especially, in the presence of titanium dioxide while in the presence of zinc oxide a plateau is reached at higher concentrations of the oxidant. Unlike hydrogen peroxide, high concentrations are not detrimental to the reaction rate and no dependence on the oxidant/contaminant molar ration is observed [27].

However, the ability of $K_2S_2O_8$ to enhance the photodegradation of parathion is not only due to the entrapment of the photogenerated electrons but also due to its own ability to absorb light and act as sensitizer through the production of sulfate radicals. Experiments with UV light and the oxidant, without the catalyst, were performed and showed that $K_2S_2O_8$ is able to cause photooxidation of the insecticide (50% degradation is achieved after 1 h of treatment). Consequently, the improvement of the photocatalytic degradation of methyl parathion by the addition of an oxidant is not only due to prevention of the recombination of the e^-/h^+ pair but also due to the photolytic activity of the oxidant. Blank experiments with the oxidant without the catalyst or UV light showed a negligible degradation of the insecticide.

3.5. Photodegradation products

Methyl parathion photocatalytic degradation yielded a number of transient organic intermediates. Up to eight transformation products have been identified using GC–MS–EI detection. The photoproducts together with their retention times and spectral characteristics are given in Table 1.

Oxidant attack of the $^{\bullet}OH$ on the P=S bond occurred first, resulting the formation of paraoxon derivative (compound **6**) which is also characteristic primary product formed during the photocatalytic degradation of other organophosphorus insecticides [11]. This is also obvious in the mineralization study (Fig. 6a) where the formation of sulfates occurs firstly in the first minutes of reaction. The continuous attack of $^{\bullet}OH$ followed by the rupture of P–O bond resulted in the formation of the corresponding phenol (compound **5**) and dialkylphosphates (compounds **1**–**4**) [28]. The formation of com-

Table 1
GC–MS–EI retention times (R_t) and spectral characteristics of identified methyl parathion photocatalytic degradation products by SPE

Compounds	R_t (min)	Characteristic ions (*m/z*)
1. *O,O*-dimethyl phosphonic ester	3.78	109, 95, 80, 79
2. *O,O,O*-trimethyl phosphoric ester	6.15	140, 110, 95, 79
3. *O,O,O*-trimethyl phosphorothioate	10.47	156, 141, 126, 110, 109, 95, 79
4. *O,O,S*-trimethyl phosphorothioate	10.61	156, 141, 126, 110, 109, 95, 79
5. *p*-Nitrophenol	22.69	139, 109, 93, 81, 65
6. Methyl paraoxon	29.54	247, 230, 109, 93, 79, 63
Methyl parathion	31.65	263, 125, 109, 93, 79, 63
7. Hydroxy methyl parathion	32.61	279, 125, 109, 93, 79, 63
8. *S*-isomer methyl parathion	35.06	263, 248, 139, 125, 79, 63

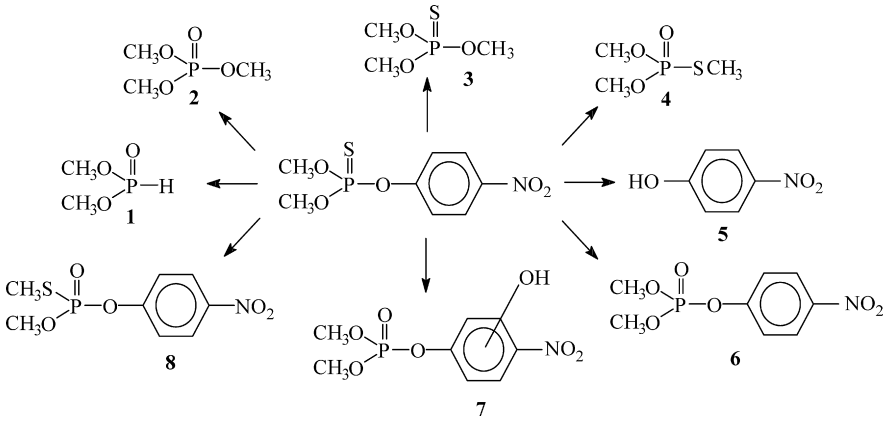

Fig. 5. Tentative photocatalytic degradation scheme of parathion methyl in TiO_2 suspensions (100 mg L^{-1}).

pounds **2**–**4** imply the transfer of methyl or methoxy groups. Compound **7** was attributed as the ring-hydroxylated derivative of parathion. It exhibits the same characteristic ions with parathion and its molecular ion M^+ at *m*/*z* 279 correspond to the addition of –OH group to the phenyl ring. Compound **8** was identified as the *S*-isomer of parathion. Its spectrum has common features with that of parathion with slightly stronger M^+ intensity, more abundant *m*/*z* 125 fragment ion, and weaker intensities in the rest common ions [29]. Especially, the main difference corresponds to the absence of the fragment ion *m*/*z* 109 which cannot be formed since the $(CH_3O)_2P(O)$ moiety does not exist. Additionally, it exhibits longer retention time than parathion. According to the above structure identification, the proposed reaction pathways for parathion methyl is shown in Fig. 5.

3.6. Mineralization

A complete degradation of an organic molecule leads to the conversion of all its carbon atoms to gaseous CO_2 and the heteroatoms into inorganic anions that remain in solution. In order to study the extend of mineralization of methyl parathion during photocatalysis, DOC measurements were carried out along with determination of the formation of inorganic ions (Fig. 6).

In the presence of TiO_2, complete disappearance of the insecticide is observed after 4 h while DOC is slightly reduced in the first 2 h indicating the formation of intermediates. At the end of treatment DOC is more than 90% reduced. Stoichiometric release of nitrate and sulfate ions is achieved after 2 and 3 h, respectively, while phosphates are formed more slowly indicating the formation of phosphate containing intermediates.

On the other hand, in the presence of ZnO, mineralization proceeds in a slower rate since DOC is only 50% reduced after 6 h of irradiation. Nitrate and sulfate ions reach only the 50 and 70% of the expected amount, respectively, while no formation of phosphates is observed even at the end of treatment. However, it is possible that phosphates are trapped by ions of zinc (due to dissolution of ZnO) to form insoluble $Zn_3(PO_4)_2$.

The addition of the oxidant (Fig. 7), although enhances the degradation of the insecticide, achieves only a slight increase to the mineralization since DOC is 95 and 70% reduced in the presence of TiO_2 and ZnO, respectively, at the end of treatment. However, in the presence of TiO_2, a different behavior of nitrates formation is observed, indicating the participation of a different oxidation mechanism.

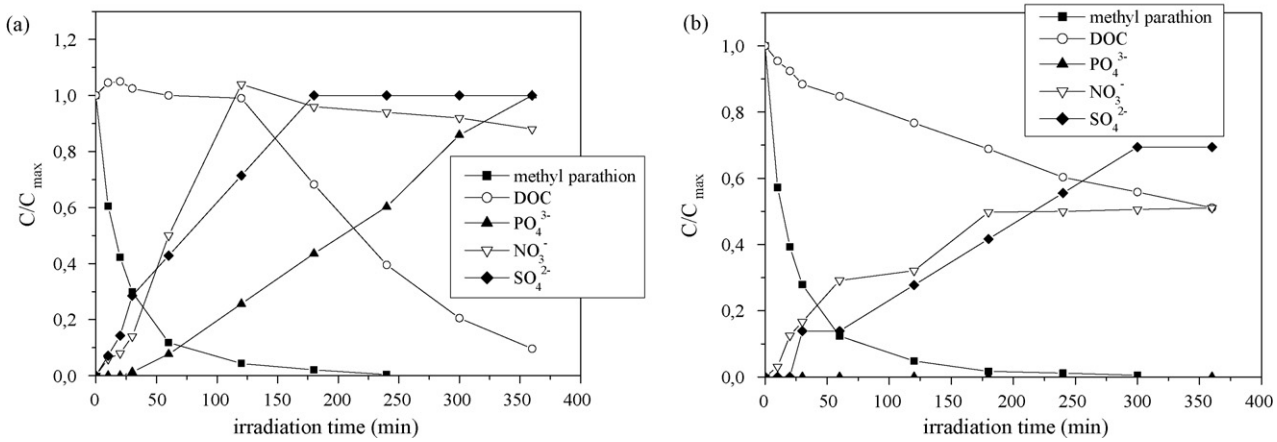

Fig. 6. Parathion/DOC reduction and SO_4^{2-}/PO_4^{3-}/NO_3^-/ release as a function of irradiation time, methyl parathion = 25 mg L^{-1}: (a) TiO_2 = 100 mg L^{-1} and (b) ZnO = 500 mg L^{-1}.

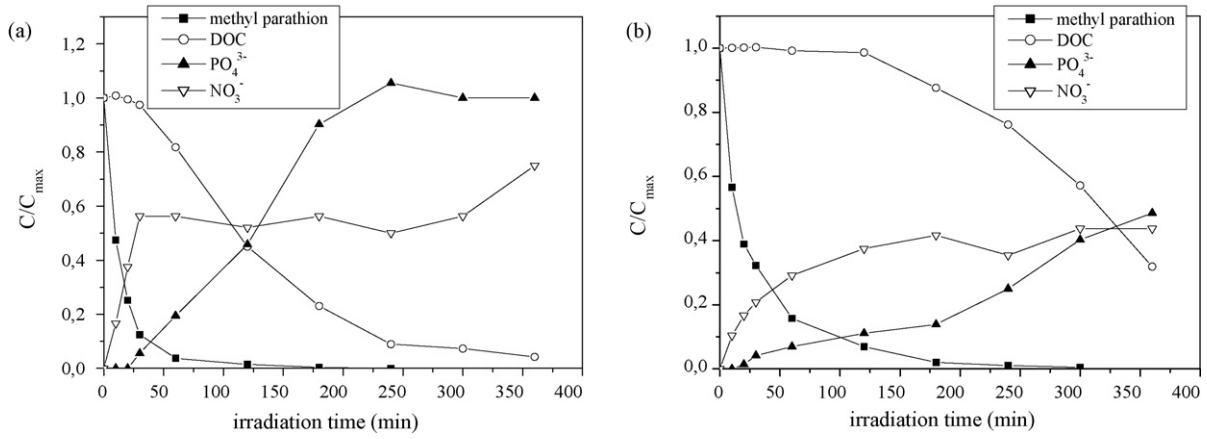

Fig. 7. Parathion/DOC reduction and PO_4^{3-}/NO_3^- release as a function of irradiation time, methyl parathion = 25 mg L^{-1}: (a) TiO_2 = 100 mg L^{-1}, $K_2S_2O_8$ = 3.1 mM and (b) ZnO = 500 mg L^{-1}, $K_2S_2O_8$ = 3.1 mM.

3.7. Toxicity measurements

The photocatalytic treatment of methyl parathion in the presence of the two semi-conducting oxides proved to be quite effective on the degradation and mineralization of the insecticide. However, when complete mineralization is not achieved, it is possible that the partial decomposition of an organic compound can lead to the formation of final products which are more toxic than the parent compound, thus, rendering toxicity measurements as an indispensable task. In our study, toxicity measurements of the treated solution were carried out in order to give a more complete evaluation of the efficiency of the technologies that have been used. In Fig. 8, changes in toxicity during the photocatalytic treatment of methyl parathion are presented.

It is obvious that variation in toxicity during treatment is dependent on the oxidation method that it is used. In the presence of titanium dioxide, a 53% reduction of toxicity was achieved while a 72% reduction was observed when the oxidant was added. Obviously, in the presence of this semiconducting oxide the toxicity is decreased during treatment which is in accordance with the mineralization of the insecticide. According to previous studies, some of the identified by-products, like the oxon derivative appear to be 10 times more toxic than the parent compound since it is a stronger acetylcholinesterase inhibitor than methyl parathion. However, the observed decrease in the toxicity is in accordance with the study of Dzyadevych and Chovelon [30] who showed that photodegradation of methyl parathion with the production of methyl paraoxon and p-nitrophenol as the main by-products caused a decrease in the toxicity since the parent compound proved to be the more toxic compound for *V. ficheri* when compared to its degradation products. Moreover, the decrease in the toxicity is also in accordance with other studies who showed that TOC is a parameter that can be easily correlated with toxicity in the case of methyl parathion since the produced intermediates are less toxic than then parent compound [12].

On the other hand, in the presence of zinc oxide toxicity is not reduced and a slight increase is observed, especially, when the oxidant is added. This increase is caused by the photodissolution of ZnO which is more intense in the presence of peroxydisulfate since sulfuric acid is produced and pH drops dramatically during photocatalysis [15]. Consequently, it is not possible to draw any conclusions concerning the toxicity of the formed photoproducts.

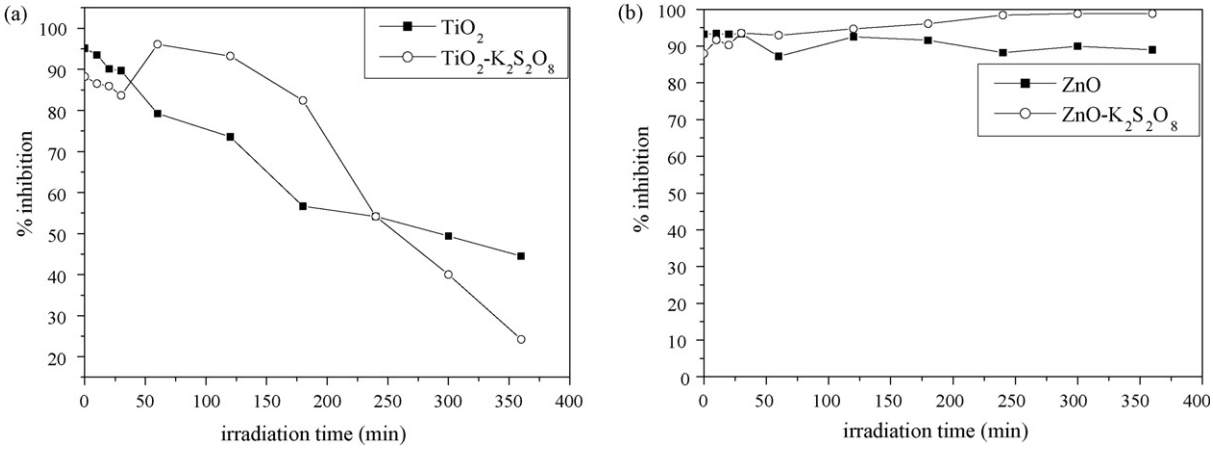

Fig. 8. Toxicity evolution as a function of irradiation time in the presence of: (a) TiO_2 = 100 mg L^{-1}, TiO_2 = 100 mg L^{-1} + $K_2S_2O_8$ = 3.1 mM and (b) ZnO = 500 mg L^{-1}, ZnO = 500 mg L^{-1} and $K_2S_2O_8$ = 3.1 mM.

4. Conclusions

The photocatalytic oxidation of methyl parathion has been studied using TiO_2 and ZnO as catalysts. Titanium dioxide proved to be more efficient photocatalyst since the oxidation and decomposition of the insecticide proceeded at higher reaction rates. Moreover, complete mineralization was achieved only in the presence of titanium dioxide. The photooxidation of the insecticide followed first order kinetics and parameters like the concentration of the catalyst play an important role affecting the reaction rate. With the addition of an oxidant into illuminated semi-conducting suspensions a synergistic effect was observed that leads to an enhancement and improvement of the efficiency of the process, achieving higher mineralization of the organic compound.

A decrease of the toxicity was observed during photocatalytic treatment with titanium dioxide suspensions in the presence or in the absence of an oxidant. On the other hand, the dissolution of zinc, in the systems with zinc oxide, did not permit to draw conclusions about the toxicity of the intermediates and final products and also raise questions regarding its use as a photocatalyst. Finally, up to eight by-products were identified during the photocatalytic degradation of methyl parathion that proceed via oxidation, hydroxylation, dealkylation and hydrolysis of the ester group reaction pathways.

Acknowledgements

This study was financed by EPEAEK under the framework of the scholarships program ‘‘HRAKLEITOS’’.

References

[1] R. Andreozzi, V. Caprio, A. Insola, R. Marotta, Catal. Today 53 (1999) 51.
[2] S. Esplugas, J. Gimenez, S. Contreras, E. Pasqual, M. Rodriguez, Water Res. 36 (2002) 1034.
[3] K. Kabra, R. Chaudhary, R. Sawhney, Ind. Eng. Chem. Res. 43 (2004) 7683.
[4] I. Konstantinou, T. Albanis, Appl. Catal. B Environ. 42 (2003) 319.
[5] M.R. Hoffmann, S.T. Martin, W. Choi, D.W. Bahnemann, Chem. Rev. 95 (1995) 69.
[6] J.-M. Herrmann, Catal. Today 53 (1999) 115.
[7] WHO, WHO guidelines for drinking water quality, third ed., Word Health Organisation (WHO/SDE/WSH/03.04/110), Geneva, 2004.
[8] K.V. Ragnarsdottir, J. Geol. Soc. 157 (2000) 859.
[9] T.-F. Chen, R.-A. Doong, W.-G. Lei, Water Sci. Technol. 37 (1998) 187.
[10] R.A. Doong, W.H. Chang, J. Photochem. Photobiol. A Chem. 116 (1998) 221.
[11] I. Konstantinou, T. Sakellarides, V. Sakkas, T. Albanis, Environ. Sci. Technol. 35 (2001) 398.
[12] T.-S. Kim, J.-K. Kim, K. Choi, M.K. Stenstrom, K.-D. Zoh, Chemosphere 62 (2006) 926.
[13] S.A. Naman, Z.A.-A. Khammas, F.M. Hussein, J. Photochem. Photobiol.: A Chem. 153 (2002) 229.
[14] E. Evgenidou, K. Fytianos, I. Poulios, Appl. Catal. B: Environ. 59 (2005) 81.
[15] E. Evgenidou, K. Fytianos, I. Poulios, J. Photochem. Photobiol. A: Chem. 175 (2005) 29.
[16] A.B. Prevot, M. Vincenti, A. Bianciotto, E. Pramauro, Appl. Catal. B: Environ. 22 (1999) 149.
[17] D. Robert, B. Dongui, J.-V. Weber, J. Photochem. Photobiol. A Chem. 156 (2003) 195.
[18] J.P. Percherancier, R. Chapelon, B. Pouyet, J. Photochem. Photobiol. A Chem. 87 (1995) 261.
[19] N. Daneshvar, D. Salari, A.R. Khataee, J. Photochem. Photobiol. A Chem. 6239 (2003) 1.
[20] S. Sakthivel, B. Neppolian, M.V. Shankar, B. Arabindoo, M. Palanichamy, V. Murugesan, Sol. Energ. Mater. Sol. C 77 (2003) 65.
[21] J.-M. Herrmann, C. Guillard, J. Disdier, C. Lehaut, S. Malato, J. Blanco, Appl. Catal. B Environ. 35 (2002) 281.
[22] I. Poulios, I. Tsachpinis, J. Chem. Technol. Biotechnol. 74 (1999) 349.
[23] I. Poulios, A. Avranas, E. Rekliti, A. Zouboulis, J. Chem. Technol. Biotechnol. 75 (2000) 205.
[24] S. Malato, J. Blanco, C. Richter, B. Braun, M.I. Maldonado, Appl. Catal. B: Environ. 17 (1998) 347.
[25] S. Irmak, E. Kusvuran, O. Erbatur, Appl. Catal. B Environ. 54 (2004) 85.
[26] M. Muneer, D. Bahnemann, Appl. Catal. B Environ. 36 (2002) 95.
[27] S. Malato, J. Blanco, M.I. Maldonado, P. Fernandez-Ibanez, A. Campos, Appl. Catal. B Environ. 28 (2000) 163.
[28] M. Kerzhentsev, C. Guillard, J.-M. Herrmann, P. Pichat, Catal. Today 27 (1996) 215.
[29] V.A. Sakkas, D.A. Lampropoulou, T.M. Sakellarides, T.A. Albanis, Anal. Chim. Acta 467 (2002) 233.
[30] S.V. Dzyadevych, J.-M. Chovelon, Mater. Sci. Eng.: C 21 (2002) 55.